

## Ferromagnetism and metallicity in $\text{Sm}_{0.2}\text{Ca}_{0.8}\text{Mn}_{1-x}\text{Ru}_x\text{O}_3$ ( $x=0-0.08$ ): Interplay between Ru doping and hydrostatic pressure

V. Markovich,<sup>1</sup> I. Fita,<sup>2,3</sup> R. Puzniak,<sup>2</sup> E. Rozenberg,<sup>1</sup> A. Wisniewski,<sup>2</sup> C. Martin,<sup>4</sup> A. Maignan,<sup>4</sup> M. Hervieu,<sup>4</sup> B. Raveau,<sup>4</sup> and G. Gorodetsky<sup>1</sup>

<sup>1</sup>*Department of Physics, Ben-Gurion University of the Negev, 84105 Beer-Sheva, Israel*

<sup>2</sup>*Institute of Physics, Polish Academy of Sciences, 02-668 Warsaw, Poland*

<sup>3</sup>*Donetsk Institute for Physics and Technology, National Academy of Sciences, R. Luxemburg str. 72, 83114 Donetsk, Ukraine*

<sup>4</sup>*Laboratoire CRISMAT, UMR 6508, ISMRA, 14050 Caen Cedex, France*

(Received 30 January 2002; published 30 May 2002)

Magnetic properties of  $\text{Sm}_{0.2}\text{Ca}_{0.8}\text{Mn}_{1-x}\text{Ru}_x\text{O}_3$  ( $x=0, 0.04, \text{ and } 0.08$ ) are investigated in the temperature range 4.2–240 K, external magnetic fields up to 15 kOe and hydrostatic pressure up to 12 kbar. Transport properties of  $\text{Sm}_{0.2}\text{Ca}_{0.8}\text{Mn}_{0.92}\text{Ru}_{0.08}\text{O}_3$  are also investigated in the temperature range 77–280 K and under pressure up to 10 kbar. It is found that for a pristine phase ( $x=0$ ), hydrostatic pressure increases the ferromagnetic domains embedded in an antiferromagnetic matrix, and slightly decreases the Néel temperature. The effect of pressure on the magnetic interactions depends upon Ru doping. For  $\text{Sm}_{0.2}\text{Ca}_{0.8}\text{Mn}_{0.96}\text{Ru}_{0.04}\text{O}_3$  an applied pressure decreases both Curie and Néel temperatures, but enhances the ferromagnetic fraction. In the case of  $\text{Sm}_{0.2}\text{Ca}_{0.8}\text{Mn}_{0.92}\text{Ru}_{0.08}\text{O}_3$  an applied pressure suppresses the ferromagnetic interactions and surprisingly increases the resistivity. To the best of our knowledge this is the first time that such an effect was observed in perovskites. All of the above observations are discussed in the context of phase separation.

DOI: 10.1103/PhysRevB.65.224415

PACS number(s): 71.30.+h; 74.62.Fj; 75.30.Kz

### I. INTRODUCTION

Numerous investigations were recently devoted to magnetic and transport properties of hole-doped Mn-based manganites with common formulas  $R_{1-x}A_x\text{MnO}_3$  ( $R$  is a trivalent rare-earth ion such as  $\text{La}^{3+}$ ,  $\text{Pr}^{3+}$ ,  $\text{Sm}^{3+}$ , or  $\text{Nd}^{3+}$ , and  $A$  is a divalent ion such as  $\text{Sr}^{2+}$ ,  $\text{Ca}^{2+}$ ,  $\text{Ba}^{2+}$ , or  $\text{Pb}^{2+}$ ). They were found to exhibit intriguing magnetic and conductive properties and characteristic colossal magnetoresistance (CMR).<sup>1</sup> Studies of these materials in the last five years have revealed a plethora of magnetic and charge-ordering structures [for example, charge/orbital ordering (CO/OO), insulating/ferromagnetic phase, charge ordered stripes etc.]. It has been established in the past that the double-exchange (DE) interaction accounts for the ferromagnetic and metallic properties of doped manganites. On the other hand, superexchange interactions cause ferromagnetic or antiferromagnetic spin ordering which may consist of insulating phases and/or charge ordering. The Jahn-Teller coupling may also play an important role in the conductivity of doped manganites.<sup>2,3</sup>

It should be noted, that in contrast to the hole-doped manganites ( $x < 0.5$ ) the electron-doped ( $x > 0.5$ ) ones have not been studied intensively. At low temperatures ferromagnetic (FM) ordering is inherent in hole-doped manganites, whereas antiferromagnetic (AFM) and insulating phases appear in electron-doped ones. The AFM ordering in electron-doped manganites attends often with charge ordering or orbital ordering.

Colossal magnetoresistance has been observed in both hole-doped and electron-doped manganite  $R_{1-x}\text{Ca}_x\text{MnO}_3$  compounds. For the latter, CMR occurs only at a very narrow composition range. For example, in  $\text{Sm}_{1-x}\text{Ca}_x\text{MnO}_3$ , the CMR effect is obtained around  $x=0.15$ , and disappears at  $x=0.20$  and  $0.10$ .<sup>4,5</sup> The magnetic, transport, and struc-

tural properties of this system were widely investigated.<sup>4–6</sup> The compound  $\text{Sm}_{0.2}\text{Ca}_{0.8}\text{MnO}_3$  (SCMO) is a  $C$ -type antiferromagnet with a Néel temperature  $T_N \approx 150$  K and a  $p$ -type conductivity at low temperatures.<sup>5</sup> It is important to note that the magnetic transition in SCMO is accompanied by a structural phase transition, from a  $P2_1/m$  structure with strong monoclinic distortion to a pure orthorhombic structure. This low-temperature magnetic structure results from a cooperative Jahn-Teller distortion of  $\text{MnO}_6$  octahedra.<sup>7</sup> A sharp increase of the conductivity occurs just above  $T_N$ . Doping of Mn sites with Ru exhibits a simultaneous development of ferromagnetic orthorhombic domains and AFM domains at low temperatures.<sup>6–8</sup> In the case  $\text{Sm}_{0.2}\text{Ca}_{0.8}\text{Mn}_{1-x}\text{Ru}_x\text{O}_3$ , low Ru doping ( $x \sim 0.1$ ) induces a FM metallic state at low temperatures and a metal-to-metal transition replacing the metal to insulator one in the pristine phase.<sup>7,8</sup> Earlier marked effects of Ru doping on the charge ordering were also found in  $\text{Nd}_{0.5}\text{Sr}_{0.5}\text{MnO}_3$ , where the ferromagnetic Curie temperature  $T_C$ , increases with Ru content and charge ordering is destroyed.<sup>9</sup>

In a previous publication<sup>10</sup> we reported on the effect of pressure on the transport properties of  $\text{Sm}_{0.2}\text{Ca}_{0.8}\text{Mn}_{1-x}\text{Ru}_x\text{O}_3$  ( $x=0$  and  $0.04$ ). Contrary to the case of pristine phase SCMO,  $\text{Sm}_{0.2}\text{Ca}_{0.8}\text{Mn}_{0.96}\text{Ru}_{0.04}\text{O}_3$  (SCMR4O) shows a CMR effect in the vicinity of the transition to AFM phase at  $T \approx 130$  K, a low time relaxation of the resistivity ( $\rho$ ), and memory effects at low temperatures.<sup>10</sup> The above effects are enhanced in a nonlinear way by external hydrostatic pressure.<sup>10</sup>

In this paper we report on our investigations of the effect of hydrostatic pressure ( $P$ ) and magnetic field ( $H$ ) on the magnetic properties of electron-doped SCMO, SCMR4O, and  $\text{Sm}_{0.2}\text{Ca}_{0.8}\text{Mn}_{0.92}\text{Ru}_{0.08}\text{O}_3$  (SCMR8O) and also on the transport properties of SCMR8O. This study is motivated by

the appearance of a magnetically phase-separated (PS) ground state of inhomogeneous OO and FM ordering,<sup>6–8</sup> developed as a result of Ru doping. Magnetic and transport measurements under pressure may shed light on the evolution and competition of different magnetic interactions in a  $\text{Sm}_{0.2}\text{Ca}_{0.8}\text{Mn}_{1-x}\text{Ru}_x\text{O}_3$  system with progressive Ru doping.

## II. EXPERIMENTAL RESULTS

The results presented in this paper were obtained on polycrystalline samples  $\text{Sm}_{0.2}\text{Ca}_{0.8}\text{Mn}_{1-x}\text{Ru}_x\text{O}_3$  ( $x=0, 0.4,$  and  $0.8$ ) prepared by a standard ceramic route. The procedures of sintering and characterization of the samples is described in Refs. 7 and 8. It involved x-ray diffraction, energy dispersive spectroscopy, and scanning electron microscopy.

Magnetic measurements under pressure were performed using a PAR Model 4500 vibrating sample magnetometer in temperature range 4.2–240 K and at magnetic fields up to 15 kOe. In this method a miniature container of CuBe,<sup>11</sup> with an inside diameter of 1.42 mm, was used as a pressure cell. The pressure at low temperatures was determined according to the known pressure dependence the superconducting transition temperature of pure tin manometer, placed near the investigated sample.

Measurements of resistivity  $\rho$  and magnetoresistance (MR) under pressure up to  $P=10$  kbar and at temperatures  $77 < T < 300$  K were carried out in another CuBe pressure cell with an inside diameter of 6 mm. The temperature in this case was measured by a Copper-Constantan thermocouple attached to the CuBe cell, and the pressure was monitored by a manganin gauge.<sup>12</sup> The decrease in pressure due to the difference in the thermal expansion of the pressure transmitting medium and the pressure cell was taken into account. Evaporated silver strips with a separation of about 1 mm between the voltage ( $V$ ) contacts were used for the customary four-point resistance measurements. In both of the above noted pressure cells, a mixture of mineral oil and kerosene was used as a pressure-transmitting medium. The MR, defined as  $[\rho(T,H) - \rho(T,0)]/\rho(T,H)$ , was measured at applied magnetic fields up to 15 kOe, oriented perpendicular to the direction of the current flow. Here  $\rho(T,H)$  and  $\rho(T,0)$  are the values of resistivity under nonzero and zero magnetic fields respectively.

Figures 1(a)–1(c) show magnetization curves for temperature and magnetic field of SCMO. The sample was cooled at zero magnetic field and the magnetization was measured upon heating and immediately thereafter upon cooling under magnetic field  $H=14.5$  kOe; see Fig. 1(a). The undoped manganite SCMO, upon cooling, exhibits a peak around 150 K consistent with the transition from semi-metallic paramagnetic (PM) phase to an AFM  $C$ -type insulating state at  $T_N=150$  K.<sup>4,7,8</sup> A significant hysteresis of about 10 K is seen in Fig. 1(a). A similar hysteretic behavior was previously found in the measurements of resistivity of SCMO.<sup>8</sup> A slight decrease of  $T_N$  as a result of applied pressure [ $dT_N/dP \approx -(0.4-0.5)$  K/kbar] is also observed in Fig. 1(a). This result fairly agrees with previous results of resistivity measurements under pressure.<sup>10</sup> Figure 1(b) shows magnetization curves vs. temperature for SCMO measured at

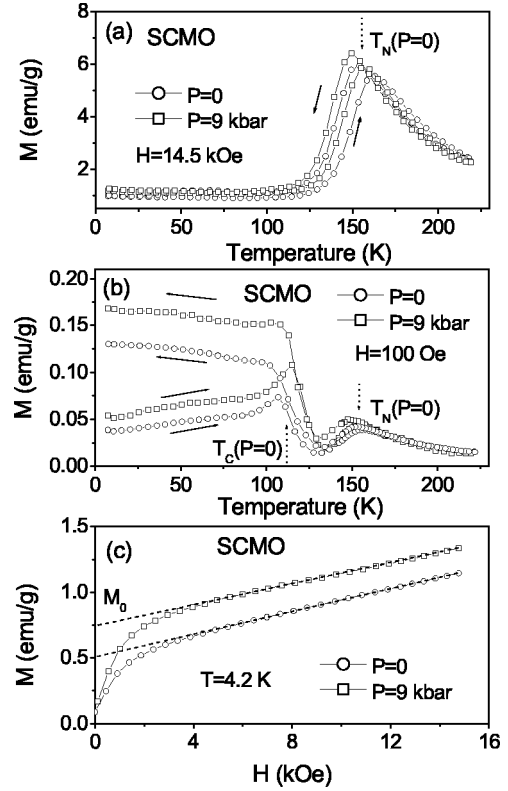


FIG. 1. Temperature dependence of the magnetization  $M$  for SCMO at ambient pressure and under pressure in magnetic field (a)  $H=14.5$  kOe; in magnetic field (b)  $H=100$  Oe. Field dependence of the magnetization  $M$  in increasing magnetic field under ambient pressure and under pressure at  $T=4.2$  K (c).

a magnetic field of  $H=100$  Oe. A wide maximum observed at  $T \approx 150$  K coincides with the PM-AFM transition, observed previously.<sup>4,7,8</sup> This maximum slightly shifts under pressure toward low temperatures. The increase of  $M(T)$  upon lowering the temperature may be associated with a ferromagnetic ordering at  $T_c \approx 115$  K ( $P=0$ ) and  $T_c \approx 118$  K under a pressure of  $P=9$  kbar; see Fig. 1(b). Below 115 K the magnetization curves upon cooling and heating exhibit a significant difference. It has already been noted that this difference is caused by the “freezing” of magnetic moments in directions energetically favored by local anisotropy and an external field, upon cooling.<sup>13</sup> Additional information on the effect of pressure on the magnetic interactions in SCMO was obtained from the field dependences of the magnetization in increasing magnetic field at  $T=4.2$  K; see Fig. 1(c). The magnetization  $M(H)$  at low magnetic fields is mainly attributed to the FM phase, whereas the AFM phase give rise to the linear high-field region. A linear extrapolation of  $M(H)$  to  $H=0$  allows us to determine the change in volume of the FM phase in respect to Ru doping and applied pressure. It appears that an applied pressure enhances the FM phase in SCMO, at  $T=4.2$  K, e.g. the FM phase of SCMO increases by about 40% in volume under pressure of 9 kbar; see Fig. 1(c).

Figure 2(a) shows magnetization curves for SCMR40 under ambient pressure and  $P=10.7$  kbar, in a magnetic field  $H=14.5$  kOe. Here again, the peak of the curves coincides

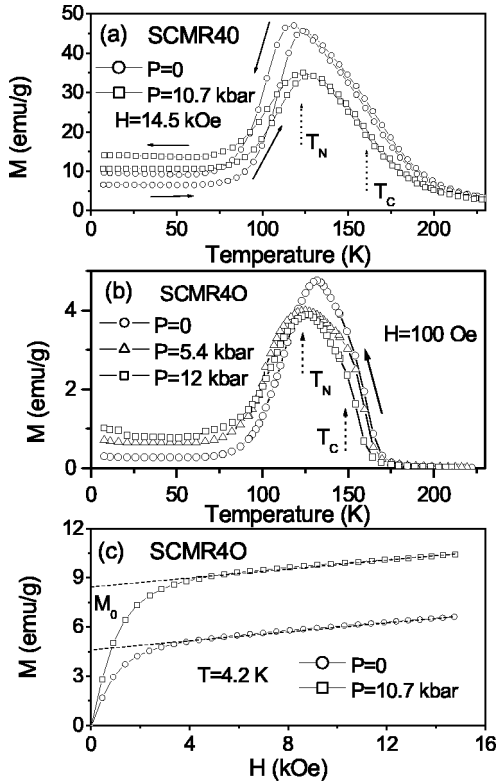


FIG. 2. Temperature dependence of the magnetization  $M$  for SCMR40 at ambient pressure and under pressure in magnetic field (a)  $H=14.5$  kOe; in magnetic field (b)  $H=100$  Oe. Field dependence of the magnetization  $M$  in increasing magnetic field under ambient pressure and under pressure at  $T=4.2$  K (c).

with a transition to the AFM phase, at  $T_N \approx 125$  K ( $P=0$ ). The values of the Curie temperature  $T_C$  were determined by the inflection point of the magnetization curves. It should be noted that the transition temperatures  $T_C$  and  $T_N$  at ambient pressure are in close agreement with the peak positions of the ac susceptibility.<sup>8</sup> Thus, starting from paramagnetic state, the Ru-doped compound becomes FM below  $T_C$  and then a coexistence of FM and AFM phases is observed below  $T_N$ .<sup>7</sup> The hysteretic behavior of SCMR40 at ambient pressure is consistent with previous results.<sup>8</sup> The effect of external pressure on the magnetization of SCMR40 is rather surprising. From Fig. 2(a), it would seem that the Curie temperature  $T_C$  decreases slightly under pressure, whereas the Néel temperature  $T_N$  increases under pressure, both with practically the same rate of (0.4–0.5) K/kbar. On the other hand, the magnetization at low temperatures under pressure increases significantly due to an increase of the volume of FM domains, at the expense of the AFM matrix. It is important to note that, according to previous resistivity measurements, the effect of pressure on  $T_N$  is opposite in sign and the value observed is  $dT_N/dP \approx -1.2$  K/kbar.<sup>10</sup> For SCMO with robust AFM phase, one may associate  $T_N$  with the maximum of low field magnetization. For the SCMR40 sample, a high enough magnetic field precludes a clear determination of the transition temperature ( $T_N$ ) to the AFM phase and the pressure dependence of  $T_N$  of this compound. Measurements of  $M(T)$  of SCMR40 were also carried out at a low magnetic

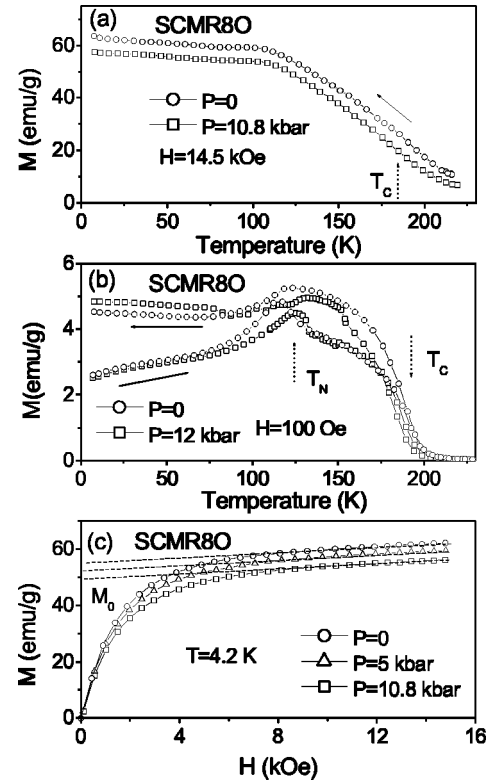


FIG. 3. Temperature dependence of the magnetization  $M$  for SCMR80 at ambient pressure and under pressure in magnetic field (a)  $H=14.5$  kOe; in magnetic field (b)  $H=100$  Oe. Field dependence of the magnetization  $M$  in increasing magnetic field under ambient pressure and under pressure at  $T=4.2$  K (c).

field  $H=100$  Oe upon heating at various pressures; see Fig. 2(b). The change of  $M(T)$  under pressure is quite unexpected. A shift downward under pressure of the positions of the inflection point ( $T_C$ ) and maximum of magnetization ( $T_N$ ) is observed. This implies that both FM and AFM interactions are reduced by external pressure. On the other hand, the increase in the magnetization at low temperatures implies an expansion of FM domains in the PS state, under pressure. Due to the proximity of FM and AFM transitions in this case, it is difficult to determine their pressure coefficients of  $T_C$  and  $T_N$ . A rough estimation shows that the pressure coefficient of Curie temperature does not exceed  $dT_C/dP \approx -(0.5-0.6)$  K/kbar. One should note that the maximum of  $M(T)$  shifts and widens in a nonlinear manner with pressure. The shift at  $P=12$  kbar does not exceed 6 K. Measurements of  $M(H)$  of SCMR40 [see Fig. 2(c)] show that applied pressure increases the volume of the FM phase, at  $T=4.2$  K. It was found that the FM phase increases by about 90% at a pressure of 10.7 kbar.

As to SCMR80 the magnetization curves vs temperature were measured at magnetic field of  $H=14.5$  kOe under ambient pressure and  $P=10.8$  kbar [Fig. 3(a)]. The inflection point of  $M(T)$  under ambient pressure practically coincides with the position of the maximum of ac susceptibility at  $T_C=190$  K.<sup>8</sup> Applied pressure leads to two remarkable effects: (i) a downward shift in the inflection point of  $M(T)$  (assigned  $T_C$ ) with pressure by  $dT_C/dP \approx -0.9$  K/kbar, thus

indicating a weakening of FM interactions under pressure; (ii) a reduction of the magnetization at low temperatures, namely, a reduction in the volume of the FM phase with pressure. It should be noted that, for SCMR80, the transition to the AFM phase at ambient pressure<sup>8</sup> is not detectable from the  $M(T)$  curve at  $H = 14$  kOe because of the predominant FM phase. The magnetization curve of SCMR80 at  $H = 100$  Oe [see Fig. 3(b)] exhibits a PM-FM transition, assigned by the inflection point at  $T_C \approx 190$  K. In addition to this the magnetization cusp about corresponds to the peak of the ac susceptibility at  $T_N \approx 115$  K found<sup>8</sup> for ambient pressure. Under an applied pressure of  $P = 12$  kbar the Curie temperature is found to be  $T_C \approx 184$  K, and  $T_N \approx 125$  K. This suggests that for SCMR80 the FM interactions are lowered by external pressure whereas the AFM ones strengthen with pressure practically with the same rate. Figure 3(c) shows curves of  $M(H)$  for SCMR80 at ambient pressure and various pressures. For SCMR80 the pressure effect is surprisingly opposite in respect to SCMO and SCMR40. It involves a decrease of  $T_C$  under pressure [see Figs. 2(a), 2(b), 3(a), and 3(b)] is of profound interest. To the best of our knowledge a positive pressure coefficient  $dT_C/dP$  was observed in all other manganite systems. The absolute value of the pressure coefficient increases with the decrease of the effective bandwidth  $W$  (Refs. 14 and 15) of the conducting electrons or, equivalently,  $T_C$ . At ambient pressure the values of the extrapolated magnetization  $M_0$  are 0.52, 4.57, and 55.3 emu/g for SCMO, SCMR40, and SCMR80, respectively. It turns out that the volume of the FM phase increases by about an order of magnitude with each 4% of Ru doping, in qualitative agreement with results published in Refs. 8 and 16.

In our previous publication<sup>10</sup> the transport properties of  $\text{Sm}_{0.2}\text{Ca}_{0.8}\text{Mn}_{1-x}\text{Ru}_x\text{O}_3$  ( $x = 0$  and 0.04) under hydrostatic pressure have been reported. Figure 4(a) shows the temperature dependence of the zero-field resistivity of SCMR80 at ambient pressure and at  $P = 9.6$  kbar. The measurements were performed upon heating. The highest-temperature gradient of the resistivity was observed in the vicinity of the Curie temperature for  $P = 0$  and 9.6 kbar. The resistivity increases under pressure in a wide temperature range below the Curie temperature, and this effect depends on temperature. The curve of resistivity vs temperature [Fig. 4(a)] shows high reproducibility at all pressures. The ratio of  $\rho(T, 0)/\rho(T, P = 9.6 \text{ kbar})$  exhibits a broad minimum in the vicinity of the magnetic transitions—see Fig. 4(b). The effect of pressure on the resistivity of ceramic samples occurs usually via the following ways: (a) An increase of the contact radius  $R$  between granules with pressure, according to  $R_P = R_0 (1 + \alpha P)^{1/3}$ ,<sup>17</sup> where  $R_0$  is the contact radius at ambient pressure and  $\alpha$  is a constant. This effect leads to the resistivity lessening under pressure. (b) An intrinsic pressure dependence of the resistivity of the sample. Contrary to numerous measurements of the resistivity of perovskite systems (including manganites)<sup>1,14,18</sup> under pressure, the resistivity of SCMR80 increases under external pressure. One can also see from Fig. 5 that an applied pressure shifts the MR minimum in the vicinity of  $T_C$  toward lower temperatures. This fact may be a circumstantial confirmation that Curie tem-

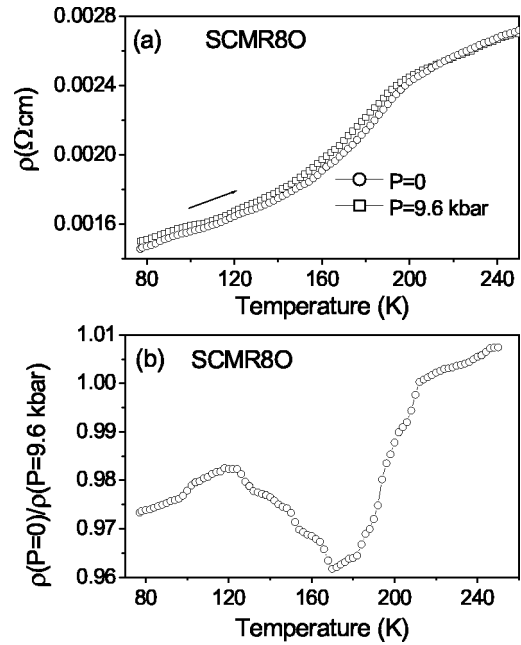


FIG. 4. Temperature dependence of the resistivity of SCMR80 at ambient pressure and  $P = 9.6$  kbar (a). Temperature dependence of the effect of pressure on the resistivity of SCMR80 (b).

perature of SCMR80 decreases under pressure. The influence of hydrostatic pressure on the MR in SCMR80 is shown in the inset of Fig. 5, which presents MR vs  $H$  at ambient pressure and  $P = 9.6$  kbar. As opposed to SCMR40,<sup>10</sup> an applied pressure practically does not affect the shape of MR of SCMR80 (see the inset of Fig. 5).

### III. DISCUSSION AND CONCLUDING REMARKS

The effect of pressure on the magnetic and structural phases for  $\text{Sm}_{0.2}\text{Ca}_{0.8}\text{Mn}_{1-x}\text{Ru}_x\text{O}_3$  ( $x = 0, 0.04$ , and 0.08) will be discussed in conjunction with the effect of Ru doping. It was already pointed out<sup>7,8</sup> that whatever is the nature

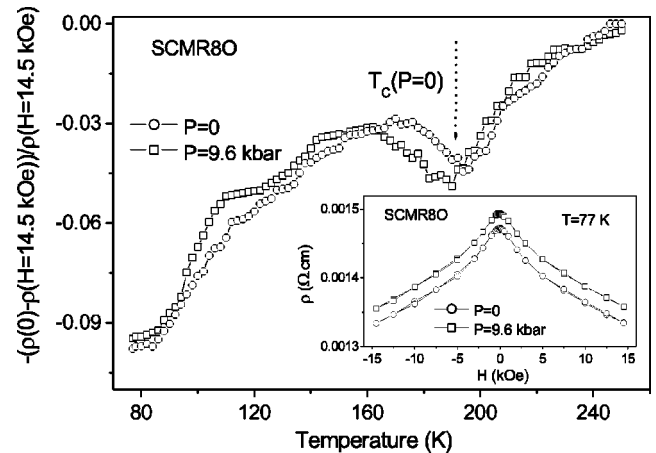


FIG. 5. Magneto-resistance of SCMR80 at  $H = 15$  kOe as a function of temperature, under ambient pressure and  $P = 9.6$  kbar. The inset shows the magneto-resistance loops of SCMR80 at ambient pressure and under  $P = 9.6$  kbar, at  $T = 77$  K.

of the initial antiferromagnetic state of undoped perovskites, ferromagnetism and metallicity can be induced by Ru doping in a manner leading to CMR properties.<sup>16</sup> In the manganese sites of the perovskites, ruthenium may exhibit two oxidation states  $\text{Ru}^{4+}$  and  $\text{Ru}^{5+}$ . It acts to increase the  $\text{Mn}^{3+}$  content in compliance with the equation  $2\text{Mn}^{4+} = \text{Ru}^{5+} + \text{Mn}^{3+}$ . Therefore,  $\text{Ru}^{5+}$  substitution enhances FM interactions between  $\text{Mn}^{4+} + \text{Mn}^{3+}$  ions via DE. Moreover, the  $\text{Mn}^{3+}$  can interact with both  $\text{Ru}^{5+}$  and  $\text{Ru}^{4+}$ -ions through a ferromagnetic superexchange interaction involving an overlap of the less than half-filled  $e_g$  orbitals of  $\text{Mn}^{3+}$  and empty  $e_g$  orbitals of  $\text{Ru}^{4+}$  and  $\text{Ru}^{5+}$ .<sup>7,8,15</sup> In addition, inherent to a pristine AFM matrix, antiferromagnetic superexchange between  $\text{Mn}^{4+}$  also operates in phase-separated Ru-doped samples.

In the case of SCMO the following transitions occurs at  $T_N = 150$  K: (i) an abrupt change of resistivity from semi-metal to insulatorlike; (ii) a monoclinic distortion from a  $Pnma$  structure and the formation of crystallographic twinning; (iii) a magnetic transition from the high-temperature PM phase to a C-type AFM state with 1D orbital ordering OO.<sup>7,16</sup> The AFM state of SCMO is extremely robust, and a strong magnetic field of more than 250 kOe is required to flip over the antiparallel spins at  $T < 100$  K (Ref. 6) and to form a FM state. Even more surprising is the revealing of a detectable FM magnetization at 4.2 K. A low value of the magnetization observed at low temperatures implies that a small enough FM phase exists in the antiferromagnetic matrix. It turns out that a PS state may exist even in the robust orbital ordered SCMO. The FM phase was also observed by measurements of electron magnetic resonance.<sup>19</sup> It was shown that applied pressure increases the volume of these FM domains at the expense of the AFM matrix [see 1(b) and 1(c)]; however on the other hand the slope of  $M(H)$  [Fig. 1(c)] depends only slightly on pressure for magnetic fields of  $H > 4$  kOe. This fact reflects the weak dependence of AFM interactions on external pressure in SCMO. In a very rough manner one may suppose that the Néel temperature is proportional to the antiferromagnetic superexchange interaction ( $J_{AF}$ ), namely,  $T_N \propto zSJ_{AF}$ , where  $z$  is the number of nearest neighbors and  $S$  is the atomic spin. Moreover, the intensity of superexchange interactions depends in a crucial way on the length and angle of the Mn-O-Mn bond. As a result, an applied pressure constitutes two somewhat independent processes, enlarging the volume of the ferromagnetic domains and slightly weakening the AFM interactions.

Doping of Mn sites with Ru leads to further development of PS, as can be seen from resistivity measurements of SCMR40.<sup>10</sup> The doping with Ru results in a redistribution of the coexisting AFM (OO) and FM domains, at  $T < T_N$ . The notable thermal hysteresis of the magnetization in SCMO and SCMR40 [Figs. 1(a) and 2(a)] is consistent with a first order of the structural transition at  $T_N$  for SCMO and SCMR40. A negligible thermal hysteresis at  $T_C$  for SCMR40 indicates that this transition is of second order. A behavior similar to that described above for SCMR40 was also observed<sup>20</sup> in  $\text{La}_{1-x}\text{Ca}_x\text{MnO}_3$  ( $x = 0.49$  and  $0.495$ ). A sharp drop of  $M(T)$  in SCMR40 [see Fig. 2(a)] at  $T_N$  is associated with a change in the magnetic interaction from double-exchange FM to superexchange AFM interaction

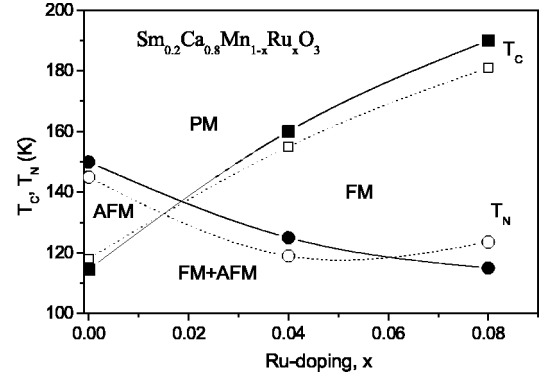


FIG. 6.  $T$ - $x$  phase diagram of  $\text{Sm}_{0.2}\text{Ca}_{0.8}\text{Mn}_{1-x}\text{Ru}_x\text{O}_3$  for  $0 < x \leq 0.08$  at ambient pressure and  $P = 10$  kbar. PM, FM, and AFM denote the paramagnetic, ferromagnetic, and antiferromagnetic phases, respectively. Here  $T_C$  is the Curie temperature and  $T_N$  is the Néel temperature. Solid lines correspond to ambient pressure, and the dotted lines represent values for  $P = 10$  kbar. All lines are guides to the eye.

when charge carriers order. A clear downward shift in temperature under pressure is observed for both transition temperatures ( $T_C$  and  $T_N$ ), implying that the external pressure weakens both FM and AFM interactions in SCMR40. It is worth noting that the resistivity does not show any real change in the vicinity PM-FM transition. In a paradoxical way the weakening of the FM interaction under pressure is accompanied by an increase of the volume of FM domains—see Fig. 2(c). The latter noted observations are consistent with the decrease of the resistivity obtained under applied pressure, at temperatures below  $T_N$ .<sup>10</sup>

As mentioned earlier, the magnetic and transport properties of SCMR80 exhibit some noticeable features. An applied pressure increases  $T_N$  and simultaneously decreases  $T_C$ , see Figs. 3(a) and 3(b). The temperature shift of the transition temperatures ( $T_C$  and  $T_N$ ) under pressure probably results from the enhancement of the AFM interactions and the weakening of the FM interactions. These effects are accompanied by a diminution of the volume of the ferromagnetic domains, and are consistent with the evolution of resistivity and magnetoresistance under applied pressure (Figs. 4 and 5).

Figure 6 presents a  $T$ - $x$  magnetic phase diagram for  $\text{Sm}_{0.2}\text{Ca}_{0.8}\text{Mn}_{1-x}\text{Ru}_x\text{O}_3$  ( $0 < x < 0.08$ ) at ambient pressure, based on the observed magnetization data. The transitions temperatures  $T_C$  and  $T_N$  coincide near  $x \approx 0.02$ . The low-temperature ground state in this figure represents the phase-separated (FM+AFM) state. Similar form of a  $T$ - $x$  magnetic phase for ambient pressure, obtained from electron magnetic resonance data, was presented recently.<sup>19</sup> The effect of hydrostatic pressure on  $T_C$  and the ferromagnetic moment  $M_0$  ( $T = 4.2$  K) for various Ru dopings is given in Fig. 7. Both  $dT_C/dP$  and  $dM_0/dP$  change in a nonlinear way with Ru doping, reflecting the competition between various magnetic interactions.

To the best of our knowledge there is a single publication<sup>21</sup> devoted to the study of pressure effect on the

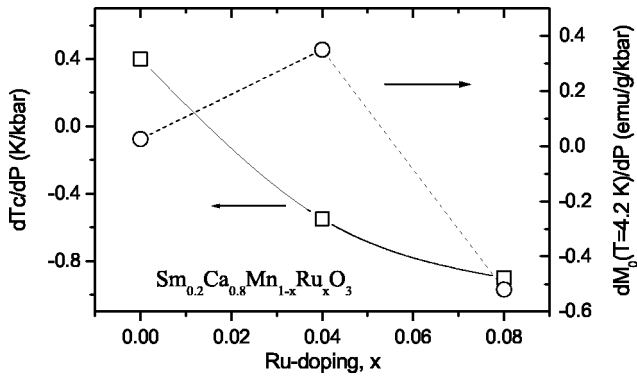


FIG. 7. Pressure coefficients of  $T_C$  and ferromagnetic moment  $M_0$  at  $T=4.2$  K for various Ru dopings. The solid line is a guide to the eye.

resistivity and  $T_C$  of electron-doped  $\text{Ca}_{1-x}\text{Y}_x\text{MnO}_3$ . Similarly to the case of hole-doped compounds, the results obtained in this case are attributed to a widening of the conduction-electron bandwidth under pressure, thereby enhancing double-exchange FM interactions. The nonlinear increase of  $T_C$  for  $\text{Ca}_{1-x}\text{Y}_x\text{MnO}_3$  ( $x < 0.2$ ) under pressure was previously discussed in the framework of competition between double exchange and AFM superexchange.<sup>21</sup>

As already stated earlier, the effect of pressure on the transport and magnetic properties of  $\text{Sm}_{0.2}\text{Ca}_{0.8}\text{Mn}_{1-x}\text{Ru}_x\text{O}_3$  system is strongly related to the content of Ru ions and phase separation. The results obtained for the magnetization and resistivity show that even the pristine  $\text{Sm}_{0.2}\text{Ca}_{0.8}\text{MnO}_3$  involves phase separation and an applied pressure may change the ratio between FM and AFM phases. Doping with Ru leads to progressive evolution of FM and AFM phases toward ferromagnetism and metallicity, corroborated by two maxima in the ac susceptibility at  $T_C$  and  $T_N$ .<sup>7,8,16</sup> It was found also that the Ru doping increases low temperature ground-state magnetization in  $\text{Sm}_{0.2}\text{Ca}_{0.8}\text{Mn}_{1-x}\text{Ru}_x\text{O}_3$  up to  $x=0.1$ .<sup>7,8,16</sup> It appears that three sorts of magnetic interactions prevail in Ru-doped samples: DE, FM superexchange, and AFM superexchange. The mutual relation between them dictates the magnetic and transport properties of Ru-doped samples. The effect of pressure depends also on specific features of the PS state. That is, in the range  $0 < x < 0.08$ , the magnetization at low temperatures increases rapidly with Ru-

doping (Figs. 1 and 2) reflecting the increase in volume of the FM phase. For SCMO and SCMR40, hydrostatic pressure acts in the usual way and enhances the volume of FM domains at the expense of the AFM phase. In the case of SCMR80 the value obtained for the low-temperature magnetization is close to the saturation value for a  $\text{Sm}_{0.2}\text{Ca}_{0.8}\text{Mn}_{1-x}\text{Ru}_x\text{O}_3$  system.<sup>8</sup> For  $0.08 < x < 0.2$  the low-temperature magnetization changes only slightly,<sup>8</sup> though it remains far enough from the spin-only moment, especially in comparison with hole-doped manganites. For example, the magnetization of  $\text{La}_{0.86}\text{Sr}_{0.14}\text{MnO}_3$  approaches the theoretical spin-only value  $3.86\mu_B/\text{Mn}$  (Ref. 22) in  $H=10$  kOe, whereas in SCMR80 it approaches the value  $1.6\mu_B/\text{Mn}$  only in  $H=14$  kOe.<sup>8</sup> Most likely, the development of the FM phase and metallicity with Ru doping depends upon a balance of the magnetic interactions, namely, DE and superexchange. In the case of SCMR80 an applied pressure tends to decrease the volume of the FM phase.

In summary, we have studied the magnetic field and pressure dependence of the magnetic and transport properties of  $\text{Sm}_{0.2}\text{Ca}_{0.8}\text{Mn}_{1-x}\text{Ru}_x\text{O}_3$  ( $x=0, 0.4$ , and  $0.08$ ). It was found that the effect of pressure on the FM and AFM interactions strongly depends on the Ru doping. For electron-doped  $\text{Sm}_{0.2}\text{Ca}_{0.8}\text{MnO}_3$  an applied pressure increases the ferromagnetic clusters embedded in robust orbital-ordered antiferromagnetic matrix, and slightly decreases the Néel temperature. For  $\text{Sm}_{0.2}\text{Ca}_{0.8}\text{Mn}_{0.96}\text{Ru}_{0.04}\text{O}_3$  an applied pressure decreases both Curie and Néel temperatures, but at the same time enhances the volume of the ferromagnetic phase. The effect of pressure on the magnetic and transport properties of  $\text{Sm}_{0.2}\text{Ca}_{0.8}\text{Mn}_{0.92}\text{Ru}_{0.08}\text{O}_3$  is strikingly different. In this case hydrostatic pressure decreases the FM interactions and the volume of the ferromagnetic phase as well. The last effect is accompanied by a prominent increase of the resistivity under pressure, which to the best of our knowledge was observed for the first time in manganites. All of above observations are discussed in the context of phase separation.

#### ACKNOWLEDGMENTS

This research was supported by the Israeli Science Foundation administered by the Israel Academy of Sciences and Humanities (Grant No. 209/01). Additional support was given by the European Community (Program No. ICA1-CT-2000-70018, Center of Excellence CELDIS).

<sup>1</sup>E. Dagotto, T. Hotta, and A. Moreo, *Phys. Rep.* **344**, 1 (2001).

<sup>2</sup>A. J. Millis, P. B. Littlewood, and B. I. Shraiman, *Phys. Rev. Lett.* **74**, 5144 (1995).

<sup>3</sup>J. S. Zhou and J. B. Goodenough, *Phys. Rev. Lett.* **80**, 2665 (1998).

<sup>4</sup>C. Martin, A. Maignan, F. Damay, M. Hervieu, and B. Raveau, *J. Solid State Chem.* **134**, 198 (1997).

<sup>5</sup>J. Hejtmanek, Z. Jirak, M. Marysko, C. Martin, A. Maignan, M. Hervieu, and B. Raveau, *Phys. Rev. B* **60**, 14 057 (1999).

<sup>6</sup>M. Respaud, J. M. Broto, H. Rakoto, J. Vanacken, P. Wagner, C. Martin, A. Maignan, and B. Raveau, *Phys. Rev. B* **63**, 144426

(2001).

<sup>7</sup>C. Autret, C. Martin, A. Maignan, M. Hervieu, B. Raveau, G. Andre, F. Bouree, A. Kurbakov, and V. Trunov, *J. Magn. Magn. Mater.* **241**, 303 (2002).

<sup>8</sup>C. Martin, A. Maignan, F. Damay, M. Hervieu, B. Raveau, and J. Hejtmanek, *Eur. Phys. J. B* **16**, 469 (2000).

<sup>9</sup>C. N. R. Rao, A. Arulraj, A. K. Cheetham, and B. Raveau, *J. Phys.: Condens. Matter* **12**, R83 (2000); P. V. Vanitha, A. Arulraj, A. R. Raju, and C. N. R. Rao, *C.R. Acad. Sci., Ser. IIC: Chim* **2**, 595 (1999).

<sup>10</sup>V. Markovich, E. Rozenberg, G. Gorodetsky, C. Martin, A. Maig-

- nan, M. Hervieu, and B. Raveau, *Phys. Rev. B* **64**, 224410 (2001).
- <sup>11</sup>M. Baran, V. Dyakonov, L. Gladczuk, G. Levchenko, S. Piechota, and H. Szymczak, *Physica C* **241**, 383 (1995).
- <sup>12</sup>V. Markovich, E. Rozenberg, G. Gorodetsky, M. Greenblatt, and W. H. McCarroll, *Phys. Rev. B* **63**, 054423 (2001).
- <sup>13</sup>D. N. H. Nam, R. Mathieu, P. Norblad, N. V. Khiem, and N. X. Phuc, *Phys. Rev. B* **62**, 1027 (2000).
- <sup>14</sup>J. M. D. Coey, M. Viret, and S. von Molnar, *Adv. Phys.* **48**, 167 (1999).
- <sup>15</sup>E. L. Nagaev, *Phys. Rep.* **346**, 387 (2001).
- <sup>16</sup>B. Raveau, A. Maignan, C. Martin, and M. Hervieu, *J. Supercond.* **14**, 217 (2001).
- <sup>17</sup>E. Z. Meilikhov, *Usp. Fiz. Nauk* **163**, 27 (1993) [*Phys. Usp.* **36**, 129 (1993)].
- <sup>18</sup>J. B. Goodenough and J. S. Zhou, *Struct. Bonding (Berlin)* **98**, 17 (2001).
- <sup>19</sup>A. I. Shames, V. Markovich, E. Rozenberg, G. Gorodetsky, A. Yakubovsky, C. Martin, A. Maignan, M. Hervieu, and B. Raveau, *J. Magn. Magn. Mater.* (to be published).
- <sup>20</sup>M. Uehara and S.-W. Cheong, *Europhys. Lett.* **52**, 674 (2000).
- <sup>21</sup>G. Garbarino, S. Paron, M. Monteverde, C. Acha, G. Leyva, D. Vega, G. Polla, J. Briatico, and B. Alascio, *J. Magn. Magn. Mater.* **226–230**, 843 (2001).
- <sup>22</sup>J. S. Zhou and J. B. Goodenough, *Phys. Rev. B* **62**, 3834 (2000).